

To be published in PRL

Strong-Pinning Effects in Low-Temperature Creep: Charge-Density Waves in TaS₃

S. V. Zaitsev-Zotov

Institute of Radioengineering and Electronics of Russian Academy of Sciences, Mokhovaya

11, 103907 Moscow, Russia.

G. Remenyi and P. Monceau

Centre de Recherches sur les Très Basses Températures, CNRS, 25, Avenue des Martyrs, BP 166

X, 38042 Grenoble Cédex, France

(February 21, 2017)

Abstract

Nonlinear conduction in the quasi-one dimensional conductor o-TaS₃ has been studied in the low-temperature region down to 30 mK. It was found that at temperatures below a few Kelvins the current-voltage (I-V) characteristics consist of several branches. The temperature evolution of the I-V curve proceeds through sequential freezing-out of the branches. The origin of each branch is attributed to a particular strong pinning impurity type. Similar behavior is expected for other physical systems with collective transport (spin-density waves, Wigner crystals, vortex lattices in type-II superconductors *etc.*) in the presence of strong pinning centers.

PACs numbers: 71.45.Lr, 72.15.Nj, 74.60.Ge, 75.30.Fv

Typeset using REVTeX

Collective transport may be observed in many physical systems such as vortex lattices in type II superconductors, electronic crystals like Wigner crystals and charge- and spin-density waves (CDW and SDW) in low-dimensional conductors, and others, as a response to an external force coupled with the respective order parameter [1,2]. The motion rate is slow down by interaction with pinning centers (impurities and imperfections) and depends also on energy dissipation, fluctuations, and other factors. In general, two limiting types of motion can be considered. In the limit of a large driving force the motion rate is controlled mostly by dissipation and fluctuations can be neglected. This regime corresponds to sliding of the spin- or charge-density waves and Wigner crystals, or to the flux-flow regime for vortex motion in type-II superconductors. In the limit of a small driving force the pinning barriers for motion are large. Motion occurs owing to rare activated overcoming of, or quantum tunneling through, pinning barriers. As a result, dissipation does not dominate any more, and fluctuations become the main factor determining the motion rate. This fluctuation-dominating regime of motion is known as the creep regime.

A quasi-one-dimensional conductor with a CDW, like TaS_3 , $\text{K}_{0.3}\text{MoO}_3$ *etc.* [1], can be considered as a model system which reveals the general properties of collective transport. At relatively high temperatures application of an electric field, E , above the threshold one, E_T , leads to the nonlinear conduction associated with sliding of the CDW. The general properties of the sliding regime are known in detail and are well understood in the framework of models considering the CDW as an elastic medium pinned by impurities [1]. At $E < E_T$ the CDW is pinned [3], and the conduction is due to normal carriers (electrons and holes) excited over the Peierls gap 2Δ and providing the activated temperature dependence of the linear conductivity $\sigma_{\parallel,\perp} \propto \exp(-\Delta/T)$, for both longitudinal, σ_{\parallel} , and transverse, σ_{\perp} , components of the conductivity tensor.

The low-temperature linear conduction indicates a contribution of a new conduction mechanism which increases σ_{\parallel} , but has no effect on σ_{\perp} . In the particular case of orthorhombic TaS_3 this contribution starts around $T = 60 - 80$ K [4], that is about one third of the Peierls transition temperature. The picture of the low-temperature nonlinear conduction

is more complex than at high temperatures and includes an additional weak nonlinearity which develops below E_T [4]. E_T grows by two-three orders of magnitude with lowering temperature down to $T = 4.2$ K, where it reaches the value of $10^2 - 10^3$ V/cm [5]. Lowering temperature makes nonlinearity at $E < E_T$ more and more pronounced and leads finally to strongly nonlinear I-V curves $I \propto (E - E_T)^\alpha$, with the exponent $\alpha = 15$ at $T = 4.2$ K [5]. Alternatively, the I-V curves can also be fitted by the exponential law $I \propto \exp[-(V_0/V)^\beta]$, with $\beta \sim 1 - 2$ [6]. The activation energies and other details of the low-temperature behavior have a large scatter and vary from sample to sample taken even from the same batch [5]. Many features of the low-temperature transport properties of quasi-one dimensional conductors like the absence of scaling of nonlinear conduction with the linear one, electric-field dependent activation energy, the exponential shape of I-V curves, temperature-dependent dielectric constant *etc.* have their natural explanation in terms of CDW creep [6–10].

In this Letter we present data on the low-temperature nonlinear conduction of TaS_3 studied in the temperature range extended down to 30 mK. It has been found that at sufficiently low temperatures the I-V curves consist of several branches. The results are described in terms of creep of the CDW pinned by strong-pinning centers.

We studied the low-temperature nonlinear conduction of four TaS_3 single crystals with different impurity contents in the temperature region down to 30 mK. Two crystals (referred hereafter as pure crystals) have the threshold field E_T for the onset of the nonlinear conduction below 1 V/cm at 100 K, and four others (impure crystals) have E_T above 10 V/cm. In addition, two other impure crystals were measured at $T > 1.5$ K.

The current-voltage characteristics were measured by the two-contact technique which is the only reliable technique for the low-temperature region, where the linear sample resistance exceeds 10^{15} Ohms. To reduce a possible contribution of contacts we studied relatively long samples with typical lengths around 5 mm. The cross-sectional area of the studied crystals was $10^2 - 10^3 \mu\text{m}^2$. Ohmic contacts were prepared by either vacuum deposition of indium, or cold soldering by indium. The shape of the I-V curves was found to be independent of the contact preparation technique.

The measurements were done using a DC voltage-control technique, and a Keithley 617 electrometer for current measurements. The data were collected from the largest to smallest voltage values. The delay between applying/changing the voltage and taking a current reading was around 1 s at relatively high currents $I > 10^{-10}$ A, and reached 30 s for currents below 10^{-13} A. From our experience such a duration was enough for the polarization current to fall below the noise level of our setup ($10^{-14} - 10^{-15}$ A). With such a delay the shape of the measured I-V curves was reproducible and independent of the direction of the voltage sweep.

The experiments below 1 K were done in a ^3He - ^4He dilution refrigerator designed especially for the low-noise electrical measurements. The samples were immersed directly in the superfluid helium of the mixing chamber. Electrical connection between the millikelvin region and the data acquisition system was provided by coaxial cables. Special attention was paid to control the Joule heating effect. The power dissipation in the samples did not exceed 10^{-11} W at 100 mK and 10^{-9} W at 1 K. The estimate of the respective Joule heating, based on the Kapitza resistance of the Cu-He boundary $R = 24$ m²K/W and $R = 2.4 \times 10^{-2}$ m²K/W for 100 mK and 1 K respectively [11] and the energy dissipations quoted above, is $\Delta T/T \sim 10^{-1}$.

Figure 1 shows a set of I-V curves taken in the temperature range 20 K - 30 mK for an impure TaS_3 sample. At temperatures above 10 K they have the usual shape reported earlier [4,5] and consist of linear and nonlinear regions. The nonlinear part can be roughly approximated by the power law $I \propto V^\alpha$ with α growing with lowering temperature. Figure 2 shows the logarithmic derivative of the I-V curves, $\alpha = d \ln I / d \ln V$, of the same sample as in Fig. 1. The linear part corresponds to $\alpha = 1$.

At temperatures below 10 K the current of the linear part is below the resolution of the measurements, and only the nonlinear part of I-V curve can be observed. A new feature of the nonlinear conduction is seen at temperatures around 10 K, where a wave-like structure is apparent on the I-V curves (Fig. 1). The existence of this structure is even more evident from Fig. 2. Up to three dips and cusps can be distinguished in $\alpha(V)$ at $T < 10$ K. This structure

can be attributed to transitions between different branches of the I-V curve; the detailed interpretation of the branches will be given in the discussion. Lowering temperature slightly shifts the structure to smaller voltages, whereas the respective currents quickly freeze out. The current of the low-voltage branches freezes out faster than that of the high-voltage ones. In other words, the temperature evolution of the I-V curves proceeds through sequential freezing-out of the branches.

The fine structure of the I-V curves reported above has been observed for all impure samples of TaS_3 . The current-voltage characteristics of pure crystals did not provide such unambiguous evidence for the fine structure, though a weak two-branch structure may be distinguished at temperatures around 10 K. No correlation between the sample sizes and the shape of the I-V curves was found. Such a dependence on impurity content and independence of the geometry proves that the fine structure results from doping rather than from possible spatial nonuniformity of the current flow in the highly anisotropic material studied. Our analysis of published results has shown that similar behavior is also present in other CDW conductors, but was overlooked by previous researchers. For example, similar wavy I-V curves can be found in published I-V curves of m- TaS_3 (see Fig. 3 of Ref. [5] at $T \leq 31.5$ K), though were not mentioned in the respective discussion. We conclude therefore that the fine structure of the low-temperature I-V curves described above is intrinsic for CDW conductors.

The behavior reported above can be understood in terms of CDW creep. In the absence of strong-pinning centers the creeping of the CDW occurs in accordance with the general scenario leading to I-V curves obeying the equation

$$j = j_0 \exp \left[-\frac{T^*}{T} \left(\frac{E_0}{E} \right)^\beta \right], \quad (1)$$

where $\beta \approx 0.5$ for 3-dimensional pinning [2]. Here j is the current density, and j_0 , T^* and E_0 will be considered below as phenomenological parameters.

Our further discussion will be based on the suggestion that samples of TaS_3 contain impurities with pinning energies high enough to provide a strong-pinning contribution [12].

The presence of strong-pinning centers is consistent with the general properties of the CDW conductors [13] and agrees with the weak-pinning effects observed at $T > 100$ K [14]. In the low-temperature region the strong-pinning centers may be responsible for the temperature-dependent maximum of the dielectric constant [7,8], for the fast mode of dielectric relaxation of the CDW [9], and for thermodynamic anomalies of CDW conductors [10].

Let us initially assume for simplicity that a sample contains only strong-pinning impurities of only one sort with pinning energy W_i (see inset in Fig. 3) and concentration n_i . For the CDW at rest ($E = 0$) the CDW phases φ at the impurity positions are suggested to be distributed uniformly in the interval $-\pi \leq \varphi \leq \pi$ [15]. In the case of unidirectional creep of the CDW, *e.g.* with positive $d\varphi/dt$, the phases tend to climb up the upward branch of the pinning potential (see inset in Fig. 3). At zero temperature and in the absence of quantum tunneling the phases reach the upper point of the pinning potential at $\varphi = \pi + \Delta\varphi_{\max}$ and then jump to the downward branch. At a finite temperature thermal fluctuations allow the barrier to be overcome before reaching the upper point. Then the upward part becomes partially empty, whereas the respective downward branch of $W(\varphi)$ is partially populated. So the center of the distribution is shifted to the right by $\Delta\varphi < \Delta\varphi_{\max}$ which gives the mean restoring force per one impurity $f = f_i \Delta\varphi/\pi$, where $f_i \approx (2\pi/\lambda)dW/d\varphi|_{\varphi=\pi}$ (see inset in Fig. 3).

Let us introduce the mean time $t_{2\pi} \equiv e\rho_e\lambda/j$ ($e\rho_e$ is the CDW charge density) corresponding to a shift of the CDW by its period, λ , and the mean time required for activation over the barrier, $t_{W_i} = t_0 \exp[W_i(E)/T]$, where t_0^{-1} is the respective attempt frequency. Then for $t_{2\pi} \gg t_{W_i}$ the barrier W_i is ineffective for pinning, so $f = 0$ and the CDW creeps in accordance with the general weak-pinning scenario [2]. A similar effect of inefficiency of the strong-pinning component is known from mesoscopic fluctuations of E_T in small samples of TaS₃ [14].

On the time scale $t_{2\pi} \ll t_{W_i}$ (i.e. at $j \gg j_{W_i} \equiv e\rho_e\lambda/t_{W_i}$) [16] the barriers smaller than $T \ln(t_{2\pi}/t_0)$ can be overcome, and impurities climb up to $\Delta\varphi = (1 - T \ln(t_{2\pi}/t_0)/W_i)\Delta\varphi_{\max}$. So at $j \gg j_{W_i}$ each impurity provides an additional force $(1 - T \ln(t_{2\pi}/t_0)/W_i)F_i$, where

$F_i = f_i \Delta \varphi_{\max} / \pi$. The electric field required for the same creep rate is then *higher* than in the weak-pinning regime by the value $E_s = (n_i F_i / e \rho_e) [1 - T \ln(j_{0i}/j + 1)/W_i]$, where $j_{0i} = e \rho_e \lambda / t_0$, and $\ln(j_{0i}/j)$ is replaced by $\ln(j_{0i}/j + 1)$ to include the case $j > j_{0i}$. Thus the resulting I-V curve consists of two branches, the weak-pinning branch obeying Eq. (1), and the similar one shifted by E_s . The growth of E leads to a gradual transition from the weak-pinning branch to the strong-pinning one. If impurities provide a variety of pinning energies W_i , then at sufficiently low temperature the I-V curve consists of several branches as shown schematically in Fig. 3 and obeys the equation

$$E = E_0 \left(\frac{T}{T^*} \ln \frac{j_0}{j} \right)^{-1/\beta} + \sum_i \frac{n_i F_i}{e \rho_e} \max \left[0, 1 - \frac{T}{W_i} \ln \left(\frac{j_{0i}}{j} + 1 \right) \right]. \quad (2)$$

Equation (2) gives the extension of Eq. (1) into the strong-pinning area. The strong-pinning effect is therefore equivalent to the appearance of a *series resistance* that *depresses* the nonlinear conduction [17] with respect to its background value provided by Eq. (1), and is ineffective at very low creep rate only. Note that tunneling through small pinning barriers W_i provides an additional channel for nonlinear conduction and may contribute to the low-temperature leveling out of $\log(I)$ *vs.* $1/T$ dependencies well known for TaS_3 below 20 K (see e.g. Refs. [4,5]).

The I-V curves of pure TaS_3 crystals at temperatures below 1 K can be fitted by Eq. (1) with $\beta = 1.5 - 2$, close to $\beta = 2$ reported for thin crystals in the quantum creep regime [6]. The general tendency of such a fit is larger β for purer crystals and lower temperatures. Thus the experimental value $\beta > 1$ is significantly higher than $\beta = 0.5$ expected for activated creep in the weak-pinning regime [2]. This discrepancy may be attributed to quantum phase slip in the bulk of a crystal [18–20], as well as to the strong-pinning effect described above. Note that the presence of strong-pinning centers could either increase the exponent β corresponding to the best fit of I-V curves, or decrease it (see Fig. 3).

In accordance with the model described above, the low-temperature transport properties of quasi-one dimensional conductors depend not only on the impurity concentration, but also on the particular impurity type. So a large variety of characteristic energies and their lack

of reproducibility noticed by a number of researchers for the low-temperature region (see e.g. Refs. [1,5]) may be due to predominance of different impurities in the different samples studied.

Summarizing, we observed fine structure in the current-voltage characteristics of TaS₃ in the CDW creep region. According to our model, this structure results from the existence of strong-pinning centers with different pinning energies. We believe that similar structure can be observed in many other physical systems where strong pinning centers are present. In particular, spin-density waves, vortex lattices in superconductors and Wigner crystals are the most probable candidates for observation of similar phenomena.

We are grateful to N. Hegman and G. Kovacs for technical assistance and help during the measurements, K. Biljaković, A. I. Larkin and V. Ya. Pokrovskii for useful discussions, and S. Brazovskii for presenting the preprint of his paper. One of us (S.V.Z.-Z.) is very grateful to CRTBT-CNRS for kind hospitality during experimental research. This work was supported by INTAS (Grant 1010-CT93-0051), and the Russian Foundation for Basic Research (Grant 95-02-05392).

REFERENCES

- [1] For a recent review see “*Charge Density Waves in Solids*”, Edited by L. P. Gor’kov and G. Gruner, Elsevier, Amsterdam, 1990, and “*Proceedings of the International Workshop on Electronic Crystals*” ECRYS’93, Edited by S. Brazovskii and P. Monceau, J. de Physique IV, **C2** (1993).
- [2] T. Nattermann, Phys. Rev. Lett. **64**, 2454 (1990).
- [3] To be specific, its better to say that thermal excitations provide much higher conduction than CDW creep.
- [4] T. Takoshima, M. Ido, T. Tsutsumi, T. Sambongi, S. Honma, K. Yamaya, and Y. Abe, Solid State Commun. **35**, 911 (1980).
- [5] M. E. Itkis, F. Ya. Nad’, and P. Monceau, J. Phys.: Condens. Matter **2**, 8327 (1990).
- [6] S. V. Zaitsev-Zotov, Phys. Rev. Lett. **71**, 605 (1993).
- [7] A. I. Larkin, Zh. Eksp. Teor. Fiz. **105**, 1793 (1994) [JETP **78**, 971 (1994)].
- [8] A. I. Larkin and S. A. Brazovskii, Solid State Commun. **93**, 275 (1995).
- [9] N. I. Baklanov and S. V. Zaitsev-Zotov, Pis’ma Zh. Eksp. Teor. Fiz. **61**, 656 (1995) [JETP Letters, **61**, 676 (1995)].
- [10] Yu. N. Ovchinnikov, K. Biljaković, J. C. Lasjaunias, and P. Monceau, Europhys. Lett. **34**, 645 (1996).
- [11] J. P. Harrison, J. Low Temp. Phys. **37**, 467 (1979).
- [12] Note that in the 3-dimensional case considered here the interaction of the CDW with impurities is characterised by two length scales. The long-range CDW distortion gives the weak-pinning contribution, whereas the local distortion may provide the strong pinning one (S. Abe, J. Phys. Soc. Jpn. **54**, 3494 (1985); **55**, 1987 (1986)).

- [13] J. L. Tucker, W. G. Lyons, and G. Gammie, Phys. Rev. B **38**, 1148 (1988).
- [14] S. V. Zaitsev-Zotov, V. Ya. Pokrovskii, and J. C. Gill, J. Phys. (France) I **2**, 111 (1992).
- [15] For the sake of simplicity we consider here only the case $T \neq 0$ and $T \ll W_i$. In this case metastable branches of the pinning potential are not populated.
- [16] Application of the electric field E tilts the energy diagram $W(\varphi)$ and decreases the maximum barrier, W_i , by $\approx (E/E_T)W_i$. We assume for simplicity that $E \ll E_T$, that is the case for the present measurements. The case $E \sim E_T$ was considered recently by Brazovskii [S. Brazovskii, in: *“Physics and Chemistry of Low-Dimensional Conductors”*, Eds. Clarie Schlenker, Jean Dumas, Martha Greenblatt, and Sander van Smaalen, NATO ASI Series, Series B: Physics, Vol. 354, Plenum NY (1996)], who found $E = E_T - C(T)[\ln(j_0/j)]^{2/3}$ for this case.
- [17] In type II superconductors the vortex lattice creep rate is coupled with E , and the mean force acting on the vortex lattice is coupled with j . So in the presence of strong-pinning impurities the I-V curve should have a similar functional form as Eq. (2) with j replaced by E and *vice versa*. Thus, in this case the strong-pining effect provides *parallel channels for conduction*.
- [18] Ji-Min Duan, Phys. Rev. B **48**, 4860 (1993); Phys. Rev. Lett. **72**, 586 (1994).
- [19] K. Maki, Phys. Lett. A **202**, 313 (1995).
- [20] H. Matsukawa, in: *“Proceedings of the 5th International Symposium on the Foundation of Quantum Mechanics in the Light of New Technology”*, Tokyo 1995 (Elsevier, to be published).

FIGURES

FIG. 1. Current-voltage characteristics of an impure TaS_3 single crystal in the temperature range 20 K - 30 mK.

FIG. 2. The logarithmic derivative $\alpha = d \ln I / d \ln V$ vs. voltage of the same sample as in Fig. 1. Broken lines mark the positions of maxima of α .

FIG. 3. I-V curve expected in the presence of strong-pinning impurities with two different pinning energies (solid line). Dotted line corresponds to the I-V curve fit by Eq. (1) with $\beta = 1/2$. Short dash line shows the best fit of $E = 1 / \ln(j) + 0.05$ with $j \propto \exp[-(E_0/E)^2]$. Inset shows the pinning energy of a strong-pinning impurity vs. the CDW phase φ . The thick line shows the phase trajectory of the strong-pinning impurity in the case of stationary CDW motion with $d\varphi/dt > 0$ at $T > 0$.

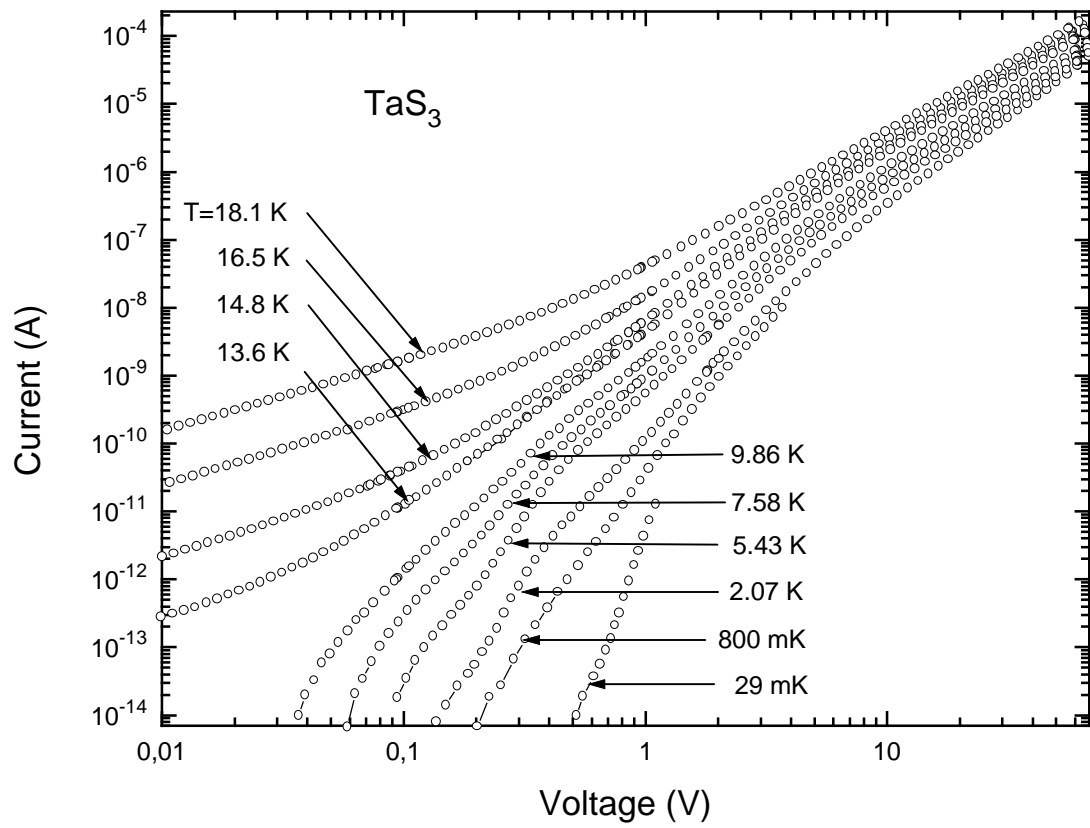


Fig. 1

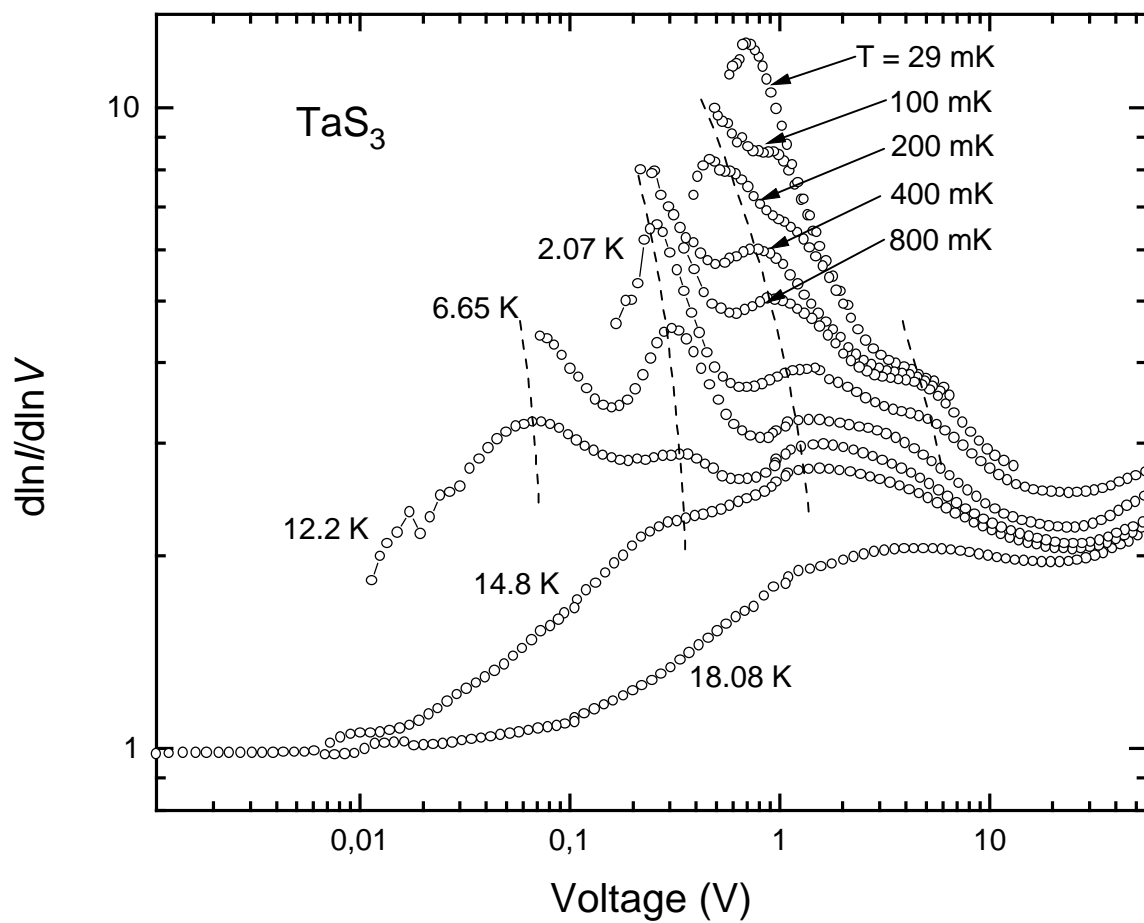


Fig. 2

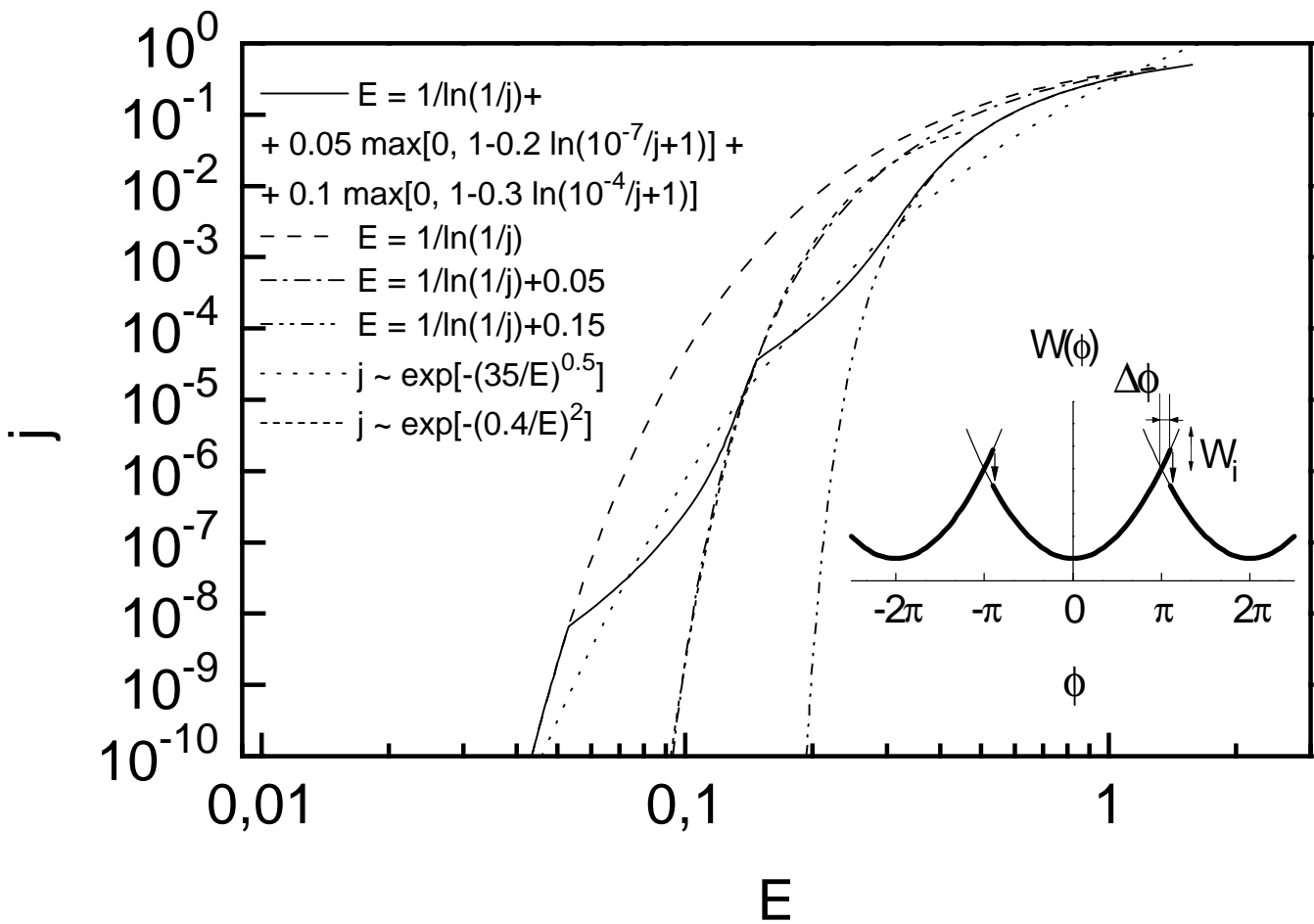


Fig. 3